Hα SURVEYS AND THE SFR DENSITY OF THE UNIVERSE

J. Gallego
Dpto Astrofísica, Universidad Complutense de Madrid, Spain.

Abstract

The measurement of the Star Formation Rate (SFR) density of the Universe as a function of look-back time is a fundamental parameter in order to understand the formation and evolution of galaxies. The current picture, only outlined in the last years, is that the global SFR density has dropped by about an order of magnitude from a peak at redshift of ∼1.5 to the current value at z=0. Using Hα luminosity as current-SFR tracer, the Universidad Complutense de Madrid (UCM) Survey provided the first estimation of the global SFR density in the Local Universe. However, the fundamental parameter that determines galactic evolution is mass, not luminosity. The mass function for local star-forming galaxies is critical for any future comparison with other galaxy populations of different evolutionary status. Besides a small fraction of 10^{11} $M_\odot$ spirals, the majority of local star-forming galaxies belong to the $<10^{10}$ $M_\odot$ category. A preliminary comparison with published data for faint blue galaxies suggests that star-forming galaxies at z=0 would have SFR per unit mass and burst strengths similar to those at z∼1, but are intrinsically less massive. Because these SFR density studies are extended to the whole range in redshift, it becomes mandatory to combine data from different SFR tracers. At low redshifts, emission lines in the optical are the most widely used. The Hα flux in emission is directly related to the number of ionizing photons and, modulo IMF, to the total mass of stars formed. Metallic lines like [OII]λ3727 and [OIII]λ5007 are affected by metallicity and excitation. Beyond redshifts z<0.4, Hα is not observable in the optical and [OII]λ3727 or UV luminosities have to be used. The UCM galaxy sample can be used to obtain a calibration between [OII]λ3727 luminosity and SFR specially suitable for the different types of star-forming galaxies found by deep spectroscopic surveys in redshifts up to z∼1.4. Recent studies based both in Hα and [OII] luminosities confirm that the SFR density of the Universe has declined dramatically since z∼1. To track this evolution into the z=1-4 regime, we must move our observational methods into the near infrared, where *JHK* imaging and spectroscopy are providing new insights into the origin and evolution of galaxies.

1 Introduction

The measurement of the Star Formation Rate (SFR) density of the Universe as a function of look-back time is a fundamental parameter in order to understand the formation and evolution of galaxies. The current picture, only outlined in the last years, is that the global SFR density observed has dropped by about an order of magnitude from a peak at redshift of $\sim$1.5 to the current value at z=0 [22] [24]. Up to date, values at z<0.4 (see Figure 2) rely on Hα luminosities [9] [31] [14] and a preliminary result using UV fluxes measured with balloon for a small sample of objects at z$\sim$0.2 [32]. For intermediate redshifts z<1 the determinations are based on broad-band continuum luminosities [21] and [OII]λ3727 luminosities [15] scaled with the SFR. Beyond z=1 UV broad-band measurements are the only SFR indicators available [22] [3] [22] [23]. Direct estimates of the SFR from a small number of galaxies detected in the infrared by ISO in the Hubble Deep Field [26] are higher than the results based in optical luminosities by a factor of five or so.

In a parallel effort, semi-analytic models developed in the last years can now predict global galaxy properties such as the Tully-Fisher relation, the B-band luminosity function, gas contents and the global evolution of the volume-averaged SFR density of the Universe at different redshifts [25] [18] [1] [27]. Most of the models reproduce the observed increase from z=0 to z$\sim$1.5, where the SFR density would decrease down to the local value at z$\sim$5. On the contrary, there is still controversy respect to the galaxy populations involved in this SFR density evolution. Some authors invoke new kind of galaxies, meanwhile others prefer mild evolution of the already known star populations (see Ellis 1998 for a nice review on this subject).

Given so many SFR tracers and indicators used for different galaxy populations, all of them have to be properly scaled and corrected for dust extinction, incompleteness, etc to provide a global picture. Any comprehensive study of global galaxy properties at high redshift have to be compared with well established local reference populations. In this way, current efforts are being oriented to obtain star-forming galaxy populations for which several different SFR estimators can be used simultaneously.

2 The SFR Luminosity Function of the the Local Universe

One of the most representative sample of current star-forming galaxies for the Local Universe is the Universidad Complutense de Madrid (UCM) Survey. The objects were selected in photographic IIIa-F objective-prism plates obtained with Schmidt Telescope via the presence of Hα+[NII]λ6584 emission in very low resolution spectra. The observational procedure and the sample of galaxies are more detailed in the discovery Lists I & II [35] [36]. Follow-up spectroscopy [10] [11] and photometry [33] [34], provide with a complete database of physical parameters for these objects.

The Hα luminosity is a very good direct measurement of the current SFR, since it is directly related to the number of massive stars (see, e.g., Kennicutt 1992). It is better than other optical Balmer lines such as Hβ or Hγ, which are more affected by stellar absorption and reddening. Metallic nebular lines like [OII]λ3727, [OIII]λ5007 (affected by excitation and metallicity), or IRAS fluxes (affected by the dust abundance and properties) are SFR indicators rather than quantitative measurements.

The UCM survey constitutes an ideal tool for studying the properties of star-forming galaxies at low redshift, since they were selected exclusively according to their Hα emission. The sample consists of about 250 sources in 500 deg^2 (z<0.045) with EW(Hα+[NII])>10Å. It is dominated by a heterogeneous population of galaxies, with 66% being intermediate to low luminosity

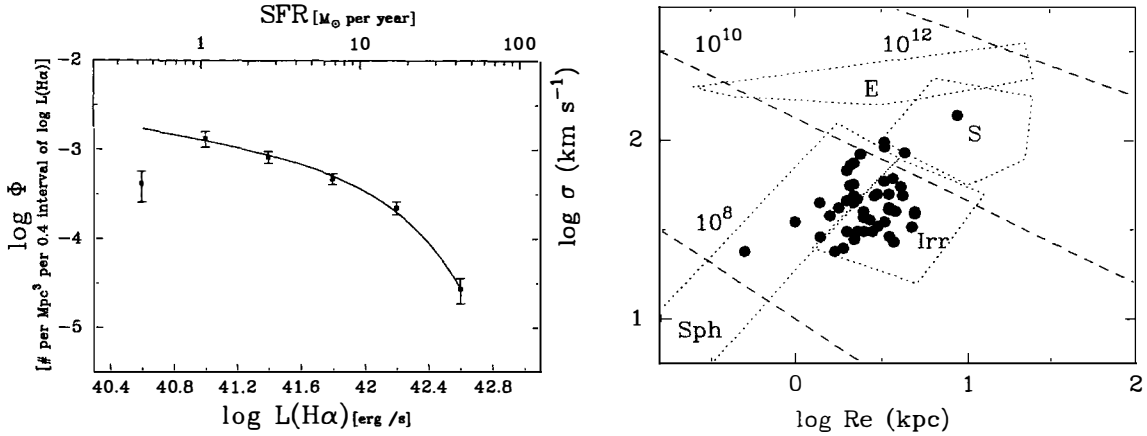

Figure 1: **Left:** Hα luminosity function for the UCM galaxies [9]. The solid line represents the best-fit Schechter function. The scale at the top of the diagram indicates the SFR corresponding for a Scalo IMF. **Right:** Half-light radius (R_e) versus velocity width (σ) diagram for some UCM local star-forming galaxies. The dashed lines correspond to constant-mass lines (in solar masses). Boundaries of typical regions occupied by different morphological types have been delimited. Sph: Spheroidals, Irr: Irregulars, S: Spirals and E: Ellipticals.

late-type galaxies. The line emission comes largely from the nuclear regions. The median luminosity is about 1 mag fainter than galaxies found in blue surveys. Up to 59% of the sample have low ionization or high extinction properties, being these galaxies difficult to identify in blue surveys for the lack of strong [OII]λ3727, Hβ or [OIII]λ5007 in emission. An aperture correction was applied to all the spectroscopic data. The observed Hα equivalent widths obtained from spectroscopy using very wide slits were transformed to total Hα luminosities scaling with the broad-band Gunn r images. Finally, observed luminosities were corrected for extinction using the Balmer decrements.

Analyzing a complete sample of emission line galaxies (ELGs) from the UCM survey, Gallego et al. (1995; [9]) computed the Hα luminosity function (see Figure 1) for the current star-forming galaxies in the Local Universe. A Schechter function with the following parameters: $\alpha = -1.3 \pm 0.2$; $L^*(\mathrm{H}\alpha) = 10^{42.15\pm0.08}\,\mathrm{erg\,s^{-1}}$ and $\phi^* = 10^{-3.2\pm0.2}\,\mathrm{Mpc^{-3}}$ for $H_0 = 50\,\mathrm{km\,s^{-1}\,Mpc^{-1}}$ provides a good fit to the present-epoch SFR function, which describes the number of star-forming galaxies as a function of their ongoing SFR. Integrating over the full range of luminosities, an Hα luminosity density of $10^{39.1\pm0.1}\,\mathrm{erg\,s^{-1}\,Mpc^{-3}}$ is obtained. Using the Hα emission as SFR estimator, this translates into a SFR density for the Local Universe of $10^{-2.4\pm0.1}\,M_\odot\,\mathrm{yr^{-1}\,Mpc^{-3}}$ in star-forming galaxies with $EW(\mathrm{H}\alpha+[\mathrm{NII}]) > 10$Å and $z < 0.045$, for a Salpeter IMF. A similar value can be derived applying a luminosity-weighted average color to the observed luminosity function in the B band, and then converting the UV flux into an instantaneous SFR. Tinsley & Danly (1980) inferred a similar density from the distribution of colors of spiral galaxies. Gronwall (1998) has also obtained a similar value from the deeper KISS survey. Despite all these results, it should be kept in mind that if some fraction of newly formed stars is completely hidden by dust, they would not contribute to the Hα luminosity, implying that the SFR derived from this quantity should be considered a lower limit.

3 Masses of the Local Star-Forming Galaxies

The major problem that arises when analyzing galactic evolution is that the fundamental parameter that determines evolution is mass, not luminosity. Pushing the idea of providing the spectroscopic surveys of distant galaxies with a reference in the local universe it is worth to carry out the estimation of masses for the star-forming galaxies of the UCM Survey. The masses of massive star-forming galaxies can be estimated via the virial theorem using the effective radius as measured in broad-band images and the velocity dispersions obtained from optical emission lines. A significative fraction of the UCM galaxies have been observed at high spectroscopic resolution (35 km s^{-1} in σ). In Figure 1 the $R_e - \sigma$ diagram for the UCM sample is shown. The zones where Ellipticals (E), spirals (S), Irregulars (Irr) and Dwarf Spheroidals (Sph) lie have been delimited. As expected, local star-forming galaxies lie on top of the distribution of spirals and Irregulars, with nearly all of them in the low mass ($<10^{10}$ $M_\odot$) region.

Despite the emission-line velocity widths could depend on the space distribution of the ionized gas and turbulence due to stellar winds, various evidences favor gravity as the mechanism that dominates the gas kinematics. Terlevich & Melnick (1981) discussed this subject and concluded that for HII galaxies the similarity of their $L - \sigma$ and $R_e - \sigma$ correlations with those of self-gravitating systems pointed to the gravitational origin. More recent models of star-forming regions [28] show that stellar winds provide an average turbulent motion similar to the velocity dispersion of the stars. Comparison between 21cm and Hα line widths further strengthens this conclusion. For a sample of 14 HII galaxies Gallego et al. (1998) derive $\langle\sigma([OIII])/\sigma(21\mathrm{cm})\rangle = 0.7 \pm 0.1$. The 30% difference may be the consequence of the larger distribution of neutral gas than for the ionized region. However, for disky objects rotation curves were utilized to compute virial masses. Similar masses have been obtained for the same galaxies from nIR broad-band observations [13]. When comparing the local data with deep Keck spectroscopy for compact star-forming systems at intermediate (0.4<z<1.4) redshift [15], star-forming galaxies at z=0 show SFR per unit mass and burst strengths similar to those at z$\sim$1, but are intrinsically less massive. These results agree qualitatively with a "downsizing" scenario, in which more massive galaxies form at higher redshift. Instead of indicating a new population of galaxies, the results suggest that these high-z star-forming objects may be related to local luminous starbursts. These results suggest an increase in the number of massive star-forming systems with redshift. To finally assess whether significant evolution has actually occurred will require more information on the relative numbers of field emission-line galaxies as a function of mass in distant and nearby galaxy samples.

4 The Hα-derived SFR Density at z$\sim$0.2

In a recent paper Tresse & Maddox (1998) used the Hα+[NII]λ6584 fluxes of the I-selected Canada-France Redshift Survey (CFRS) galaxies lying at a redshift z below 0.3 to derive the Hα luminosity function. The CFRS survey is a magnitude limited (M_B>-21 mag for z<0.3) sample fairly representative of field galaxies. Because of the I-band selection, the galaxies have been selected by light from the old stellar population ,rather than on their young stars. Consequently, the CFRS sample is less sensitive to recent star formation than Hα selected samples. Due to the low dispersion of the spectroscopic data an average correction for the [NII]λ6584 was used. An aperture correction based in the V-band flux and an average extinction correction (except for a fraction of objects with Hβ detected) were applied. A Schechter function provides a good fit with the following parameters: $\alpha = -1.35 \pm 0.06$; $L^*(\mathrm{H}\alpha) = 10^{42.13\pm0.13}\,\mathrm{erg\,s^{-1}}$ and $\phi^* = 10^{-2.8\pm0.1}\,\mathrm{Mpc^{-3}}$ for $H_0 = 50\,\mathrm{km\,s^{-1}\,Mpc^{-1}}$. They obtained a total Hα luminosity

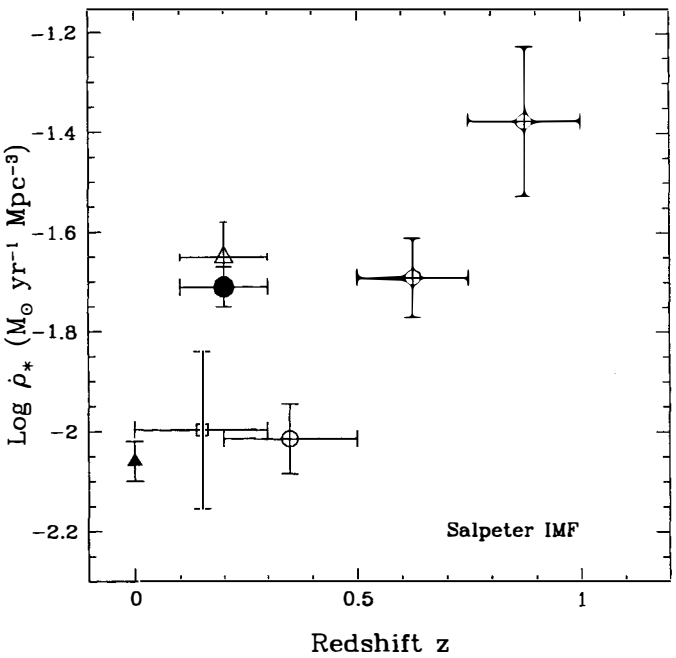

Figure 2: Volume-averaged SFR versus redshift [31]. Open circles are from UV(2800 Å) CFRS data [21], open square is from UV(2000 Å) data of Treyer et al. (1997), the filled triangle is from local Hα data [9], whereas the filled circle corresponds to Hα CFRS data [31] that converts on the open star when the faintest Hα luminosity bin of the CFRS data is included. Note that Hα data are reddening corrected, while UV data are not.

density of at least $10^{39.44\pm0.04}$ erg s^{-1} Mpc^{-3} at a mean z=0.2 for galaxies with rest-frame EW(Hα+[NII]) > 10Å. This is twice the value found in the local Universe by Gallego et al. (1995).

They have also obtained that at least ~40% of the ELGs present in the sample are relatively red galaxies that contribute to the overall luminosity as well as the blue galaxies. Most of these objects are spiral galaxies and correspond to Starburst nuclei (SBN) and Dwarf Amorphous Nuclear Starbursts (DANS [10]). However, meanwhile AGNs where removed from the UCM sample, Hammer et al. (1997) conclude that a large fraction of the z<0.3 CFRS galaxies are low-luminosity objects with AGN activity.

The discrepancy observed in Figure 2 between UV and Hα data can be solved assuming a dust extinction correction of $\sim$ 1 mag for the UV data. Finally, when combining the z=0 and z$\sim$0.2 values, the Hα SFR evolution seems to follow a $(1+z)^3$ law. This behavior is confirmed using [OII]λ3727 luminosities for the CFRS galaxies by Hammer et al. (1997), by Hogg et al. (1998) for the Caltech Faint Galaxy Redshift Survey and by Cowie et al. (1997) for the Hawaii Redshift Survey.

5 Star Formation Rate Tracers up to z∼0.4

Because the UV continuum emission from a galaxy with significant ongoing star formation is dominated by hot stars, the unreddened UV luminosity scales (modulo IMF) very well with the current SFR of the burst, independently of the past star formation history. This UV continuum, usually measured at 1500Å , 2000Å or 2800Å, lies in the optical for intermediate to high redshift objects but is not easily measurable for low redshift objects. For Salpeter IMF

$$L_{\mathrm{UV(2800)}} = 8.0 \times 10^{27} \left(\frac{\mathrm{SFR}}{\mathrm{M_\odot\ yr^{-1}}} \right) \mathrm{erg\ s^{-1}\ Hz^{-1}} \quad (1)$$

The Hα luminosity, related to the Lyman-continuum flux of the embedded stars, is also a direct measurement of the current SFR modulo the IMF [19] [20]. Assuming case-B recombination theory and a Salpeter IMF function (the coefficient for a Scalo IMF is 3.3 times smaller), the Hα luminosity scales with the SFR as

$$L_{\mathrm{H}\alpha} = 1.5 \times 10^{41} \left(\frac{\mathrm{SFR}}{\mathrm{M_\odot\ yr^{-1}}} \right) \mathrm{erg\ s^{-1}} \quad (2)$$

Despite the Hα line is one of the most reliable indicators of SFR, it is observable in the optical only out to redshifts z<0.4. In order to compare in a direct way the results in Hα for local samples and the results in UV luminosity for z>0.4 star-forming galaxies, several SFR indicators have been considered. Far infrared fluxes are heavily affected by dust abundance and properties and, moreover, they are not easily observable for high-z sources. The decimetric radio continuum has been recently proposed as an useful SFR tracer [6]. It appears to be directly proportional to the rate of formation of supernovae in a galaxy. Despite it shows a good concordance with SFR estimated from U-band, Hα and infrared luminosities, serious discrepancies have been found.

Despite metallic nebular lines such as [OII]λ3727 and [OIII]λ5007 are affected by excitation and metallicity, they could be used as SFR indicators when the population of galaxies used for the calibration is similar to the one we want to study [8] [20]. Figure 4 shows the relation between the equivalent widths of the [OII]λ3727 and [OIII]λ5007 versus Hα+[NII]λ6584 for the whole UCM sample of galaxies. The symbols correspond to low-ionization StarBurst Nuclei (SBN) galaxies and Dwarf Amorphous Nuclear Starbursts (DANS [10]) and high-ionization HII-like Blue Compact Dwarfs (BCD) and HII galaxies. There is an acceptable correlation between [OIII] and Hα+[NII] for the strongest emission-line galaxies but it becomes very loose for the SBN-like objects. It is worth notice that a total fraction of 29% of objects with normal ongoing star formation show no [OIII]λ5007 in emission at all. Even worse, the HII-like and SBN-like objects present a different behavior that forces the classification of the object before applying any SFR calibration.

The [OII]λ3727 emission line is the most useful star formation tracer in the blue optical. Figure 4 shows the relation between the [OII] and Hα+[NII] EWs for UCM galaxies. All the star-forming galaxies follow a mean relation EW([OII]) = 0.2 EW(Hα+[NII]). Still a fraction of mainly SBN-like galaxies show no [OII]λ3727 emission at all but their contribution is in average ∼26% of the total amount.

The most promising property of the [OII]λ3727 is that it is observable in the optical up to z∼1.4. In this way, the [OII] luminosity provides with a useful SFR calibration for distant star-forming galaxies. If we assume that Hα luminosity scales with the [OII] luminosity, the calibration between SFR and Hα can be transformed to [OII] luminosity. Using the UCM galaxies database we obtain the following general relation

$$\mathrm{SFR\ M_\odot\ yr^{-1}} = 8.1 \times 10^{-41}\ \mathrm{L_{[OII]}\ erg\ s^{-1}} \quad (3)$$

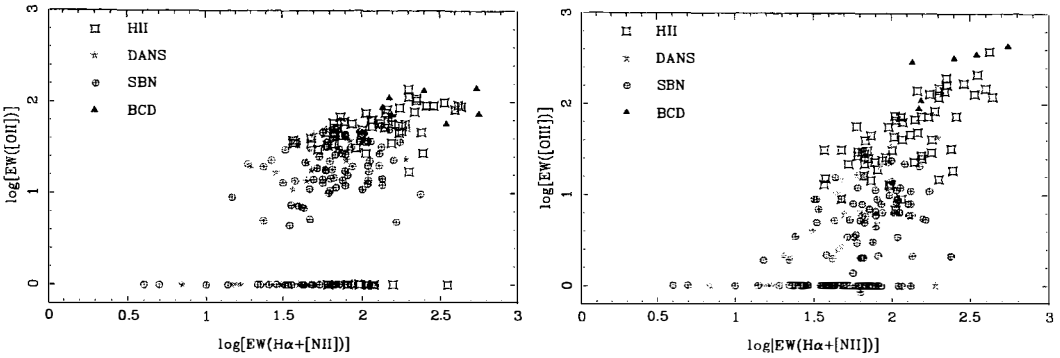

Figure 3: Relation between the equivalent widths of the [OII]λ3727 and [OIII]λ5007 lines versus Hα+[NII] for UCM galaxies. Symbols follow the Gallego et al. (1996) classification, with HII for HII galaxies, DANS for Dwarf Amorphous Nuclear Starbursts, SBN for Starburst Nuclei and BCD for Blue Compact Dwarf galaxies. Note the significative fraction of star-forming objects detected in Hα with no emission in the blue.

A tighter correlation can be obtained if we split the total sample of star forming galaxies into two main classes for red objects (SBN-like) and blue galaxies (HII-like). For this analysis, all UCM ELGs that are spiral galaxies that host a nucleus with an star-forming process and low ionization and dim or null emission lines in the blue classify as SBN-like objects. Bluer objects, with strong [OIII]λ5007 in emission and compact or idly defined morphologies classify as HII-like objects. The corresponding calibrations are

$$\mathrm{SFR_{SBN}\ M_\odot\ yr^{-1}} \ = \ 7.9 \ \times \ 10^{-41}\ \mathrm{L_{[OII]}\ erg\ s^{-1}} \tag{4}$$

$$\mathrm{SFR_{HII}\ M_\odot\ yr^{-1}} \ = \ 9.9 \ \times \ 10^{-41}\ \mathrm{L_{[OII]}\ erg\ s^{-1}} \tag{5}$$

Gallagher et al. (1989) and Kennicutt (1992) also derived SFR calibrations for L([OII]) based on spectrophotometry of blue irregular and normal spiral galaxies respectively. The first one is close to the obtained for HII-like galaxies. The second one is close to the one obtained for SBN-like galaxies. In order to avoid flux calibrations and provide a calibration suitable for redshift surveys of distant galaxies a relation between blue absolute magnitude M_B, [OII]λ3727 luminosity and [OII]λ3727 equivalent width can be introduced.

$$\mathrm{SFR_{SBN}\ M_\odot\ yr^{-1}} \ \sim \ 8.2 \times 10^{-12} \times 10^{-0.4\,(M_B - M_{B\odot})}\ EW_{\mathrm{[OII]}} \tag{6}$$

$$\mathrm{SFR_{HII}\ M_\odot\ yr^{-1}} \ \sim \ 10.2 \times 10^{-12} \times 10^{-0.4\,(M_B - M_{B\odot})}\ EW_{\mathrm{[OII]}} \tag{7}$$

These expressions are $\sim$1.1 and $\sim$1.25 times larger than that derived by Kennicutt (1992), $\sim$6 times larger than that obtained by Gallagher et al. (1989) and $\sim$4 times larger than that used by Guzmán et al. (1997) for compact galaxies in the HDF. The dispersion in the main correlations introduces a significant error that is amplified by the errors inherent to the [OII]λ3727 flux itself as SFR tracer. Hammer et al. (1997) already pointed out that the Kennicutt (1992) calibration, when applied to CFRS sample, would predict more mass in the form of stars that the quantity observed in the Local Universe. Hence the SFRs derived from the previous equations should be considered as rough but useful estimates.

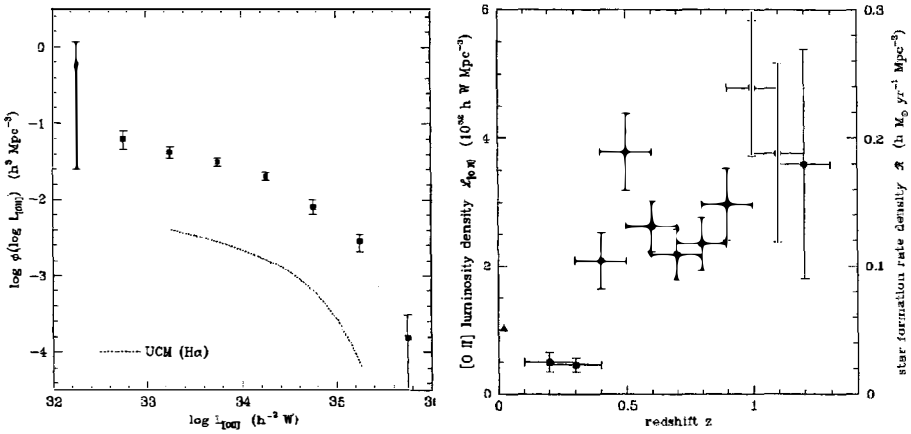

Figure 4: **Left:** The [OII]λ3727 luminosity function for the Caltech Faint Galaxy Redshift Survey ([17], see text). The dotted line shows the Gallego et al. (1995) Hα luminosity function for the UCM survey. It has been converted to [OII] luminosities applying a constant $L_{[OII]}/L_{H\alpha}$=0.46. **Right:** [OII]λ3727 luminosities and SFR densities for the Caltech sample [17]. For reference, the Gallego et al. (1995) value is shown as a solid triangle. $H_0 = 100\,\mathrm{km\,s^{-1}\,Mpc^{-1}}$.

6 The Evolution of the [OII]λ3727 and Hα Density of the Universe

Several authors have applied to the spectroscopic data obtained from deep redshift surveys a calibration between SFR and [OII]λ3727 luminosity similar to the one obtained in the previous section. Hogg et al. (1998) have applied the Kennicutt (1992) calibration to the galaxies of the Caltech Faint Galaxy Redshift Survey. It corresponds to a sample of 375 galaxies (~75% spectroscopically complete) down to R=23.3 eight arc-minutes around the HDF. They used the [OII]λ3727 equivalent widths, R fluxes and spectral energy distributions (from R-K color) to estimate the [OII] luminosity. The [OII] luminosity function for the entire sample in the redshift range 0<z<1.5 is compared with the local function in Figure 4. The UCM values have been multiplied by a factor of 0.46 taken from Kennicutt (1992) to translate the Hα values to [OII] luminosities. Overall, the line luminosity is higher by an order of magnitude in the higher-redshift sample. The [OII] luminosity density as a function of redshift for different binnings is also shown in Figure 4 (Filled star at z=1 in Figure 5). Despite the UCM value appears higher than the Hogg et al. (1998) estimations at z~0.3 due to a strong incompleteness of the faint sample, at z=0.4 an increase by a factor of x2 is again recovered. At z~1 it seems that optical estimations can not reproduce the SFR densities inferred from UV luminosities.

Figure 5 represents all the most important observations and data sets to date. Lilly et al. (1996; open circles) UV luminosities for the CFRS sample and Madau (1996; arrows) UV luminosities for the HDF have been also plotted for reference. Guzmán et al. (1997) applied their own calibration to the data set of Cowie et al. (1995; stars in Figure 5), which corresponds to a Keck spectroscopic survey ~90% complete down to I_{AB}<22.5. Up to z~1, where incompleteness affects more seriously to the data, the general increase observed for the CFRS sample using UV luminosities [21] is confirmed. Moreover, they follow very tightly a general relation

$$SFR \sim (1+z)^3 \tag{8}$$

Cowie et al. (1997) analyzed an extended to B<24.5 redshift sample to study the evolution

of the SFR luminosity function. Correcting for the different SFR-[OII]λ3727 luminosity their results are consistent with a SFR density for the 0.1-0.4 redshift range as twice the Gallego et al. ([9] filled triangle at z=0) value for the Local Universe. this x2 increase is in agreement with the one obtained by Guzmán et al. (1997) and Tresse & Maddox (1998; filled triangle at z=0.2).

Hammer et al. (1997) applied the Kennicutt (1992) calibration to study the SFR density evolution from the [OII]λ3727 luminosity density of the CFRS sample. They found an increase for field galaxies at z=0.375 of a factor 1.6 respect to the Gallego et al. (1995) value, and a factor of 8.4 between z=0.375 and z=0.85. The latter increase is even larger than the one obtained at 2800 Å by Lilly et al. (1996), although the overall increase over the whole redshift range from z=0 to z=1 is comparable. The UV luminosities obtained by Lilly et al. (1996) for the CFRS sample are observed values. It is necessary to apply 1 mag correction for extinction to recover the Hammer et al. (1997) luminosity densities. Photometric redshifts applied to the HDF [3] are in agreement the scenario exposed above.

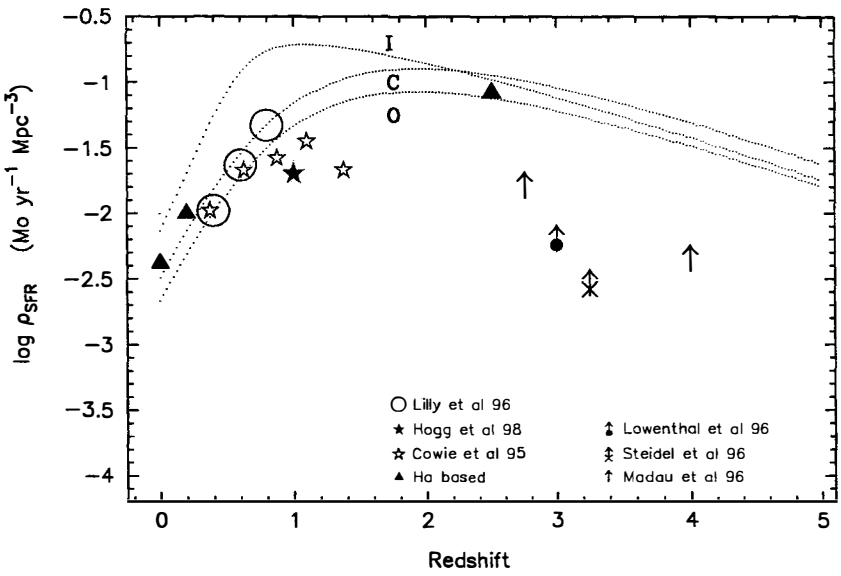

Figure 5: Comoving-volume averaged current SFR density as a function of redshift (Salpeter IMF, q_o=0.5 and $H_0 = 50\,\mathrm{km\,s^{-1}\,Mpc^{-1}}$ cosmology). The dotted lines represent Pei & Fall (1995) models. C=Closed box model, I=Inflow of metal-free gas and O=Outflow of metal-enriched gas model. Errors bars have been omitted for clarity. See text for description of the various data sets.

Finally, Bechtold (1998) have carried out a spectroscopic survey in the near infrared looking for Hα from high redshift galaxies. Using the IRTF and Palomar 5m nIR cameras they have detected a population of Hα emitters at z$\sim$2.5. Despite the spectroscopic confirmation is still in the way, preliminary results based on the Hα flux observed in tuned nIR narrow band images are very promising. It means a SFR density at z$\sim$2.5 (filled triangle at z$\sim$2.5 in Figure 5) roughly 20 times larger than the local value. This result is consistent with the results derived from UV luminosities by Madau et al. (1996). Combining future observations in the near infrared with data sets selected by their Hα luminosities at low and moderate redshifts will allow a coherent check on the Star Formation Rates of the Universe derived from other means.

References

[1] Baugh, C.M., Cole, S., Frenk, C.S., Lacey, C.G., 1998, *Astrophys. J.* **498**, 504

[2] Bechtold, J., 1998, in The Young Universe, ASP Conference Series, **146**

[3] Connolly, A.J., Szalay, A.S., Dickinson, M.E. et al., 1997, *Astrophys. J.* **486**, L11

[4] Cowie, L.L., Hu, E.M., Songaila, A., 1995, Nature **377**, 603

[5] Cowie, L.L., Hu, E.M., Songaila, A., 1997, *Astrophys. J.* **481**, L9

[6] Cram, L., Hopkins, A., Mobasher, B., Rowan-Robinson, M., 1998, in press astro-ph/9805327

[7] Ellis, R.S., 1998, ARA&A in press

[8] Gallagher, J.S., Bushouse, H., Hunter, D.A., 1989, *Astron. J.* **97**, 700

[9] Gallego J., Zamorano J., Aragón-Salamanca A., Rego M. 1995, *Astrophys. J.* **455**, L1

[10] Gallego J., Zamorano J., Rego M., et al., 1996, *Astr. Astrophys.* **120**, 323

[11] Gallego J., Zamorano J., Rego M., Vitores A.G. 1997, *Astrophys. J.* **475**, 502

[12] Gallego J., Guzmán, R., Koo, D.C., Salzer, J.J., 1998, *Astrophys. J.* , in prep

[13] Gil de Paz, A., Zamorano, J., Gallego J, 1998, *Astrophys. J.* , in prep

[14] Gronwall, C., 1998, this volume

[15] Guzmán, R., Gallego, J., Koo, D.C. et al., 1997, *Astrophys. J.* **489**, 559

[16] Hammer, F., et al., 1997, *Astrophys. J.* **481**, 49

[17] Hogg, D.W., Cohen, J.G., Blandford, R., Pahre, M.A., 1998, *Astrophys. J.* **in press**, astro-ph/9804129

[18] Kauffmann, G., Nusser, Steinmetz, 1997,

[19] Kennicutt, R.C., 1983, *Astrophys. J.* **272**, 54

[20] Kennicutt, R.C., 1992, *Astrophys. J.* **388**, 310

[21] Lilly, S.J., Le Fevre, O., Hammer, F., & Crampton, D., 1996, *Astrophys. J.* **46**, L1

[22] Madau, P., Ferguson, H.C., et al., 1996, *MNRAS* **283**, 1388

[23] Madau, P., 1997a, in SF Near and Far, ed. Holt & Mundy, astro-ph/9612157

[24] Madau, P., 1997b, in The Hubble Deep Field, ed. M. Livio, S. M. Fall, & P. Madau, STScI Symposium Series, astro-ph/9709147

[25] Pei, Y.C., Fall, S.M., 1995, *Astrophys. J.* **454**, 69

[26] Rowan-Robinson, M., et al., 1998, *MNRAS* **289**, 490

[27] Somerville, R.S., Primack, J.R., 1998, *MNRAS* **in press**, astro-ph/9802268

[28] Tenorio-Tagle, G., Muñoz-Tuñón, C., & Cox, D.P., 1993, *Astrophys. J.* **418**, 767

[29] Terlevich, R., Melnick, J., 1981, *MNRAS* **195**, 839

[30] Tinsley, B.M., Danly, L., 1980, *Astrophys. J.* **242**, 435

[31] Tresse, L., Maddox, S.J., 1998, *Astrophys. J.* **495**, 691

[32] Treyer, M.A., Ellis, R.S., et al., 1997, in The UV Universe at Low and High Redshift, ed. Walker (Woodbury AIP Press), in press.

[33] Vitores A.G., Zamorano J., Rego, et al., 1996a, *Astr. Astrophys. Suppl. Ser.* **118**, 7

[34] Vitores A.G., Zamorano J., Rego, et al., 1996b *Astr. Astrophys. Suppl. Ser.* **120**, 385

[35] Zamorano J., Rego M., Gallego J., et al., 1994, *Astrophys. J.* **95**, 387

[36] Zamorano J., Gallego J., Rego M., et al., 1996, *Astrophys. J. Suppl. Ser.* **105**, 343